Journal of Magnetic Resonance 199 (2009) 242–246

Contents lists available at ScienceDirect

Journal of Magnetic Resonance

journal homepage: www.elsevier.com/locate/jmr

Communication

Structural analysis of uniformly ^{13}C-labelled solids from selective angle measurements at rotational resonance

Simon G. Patching [b], Rachel Edwards [a], David A. Middleton [a,*]

[a] School of Biological Sciences, University of Liverpool, Crown Street, Liverpool L69 7ZB, United Kingdom
[b] Astbury Centre for Structural Molecular Biology and Institute of Membrane and Systems Biology, University of Leeds, Leeds LS2 9JT, United Kingdom

ARTICLE INFO

Article history:
Received 5 March 2009
Revised 24 April 2009
Available online 9 May 2009

Keywords:
Rotational resonance
Dipolar coupling
Cross-polarization magic-angle spinning
Double-quantum filter
Uridine
Valine

ABSTRACT

We demonstrate that individual H–C–C–H torsional angles in uniformly labelled organic solids can be estimated by selective excitation of ^{13}C double-quantum coherences under magic-angle spinning at rotational resonance. By adapting a straightforward one-dimensional experiment described earlier [T. Karlsson, M. Eden, H. Luhman, M.H. Levitt, J. Magn. Reson. 145 (2000) 95–107], a double-quantum filtered spectrum selective for Cα and Cβ of uniformly labelled L-[^{13}C,^{15}N]valine is obtained with 25% efficiency. The evolution of Cα–Cβ double-quantum coherence under the influence of the dipolar fields of bonded protons is monitored to provide a value of the Hα–Cα–Cβ–Hβ torsional angle that is consistent with the crystal structure. In addition, double-quantum filtration selective for C6 and C1′ of uniformly labelled [^{13}C,^{15}N]uridine is achieved with 12% efficiency for a ^{13}C–^{13}C distance of 2.5 Å, yielding a reliable estimate of the C6–H and C1′–H projection angle defining the relative orientations of the nucleoside pyrimidine and ribose rings. This procedure will be useful, in favourable cases, for structural analysis of fully labelled small molecules such as receptor ligands that are not readily synthesised with labels placed selectively at structurally diagnostic sites.

1. Introduction

NMR methods for restoring rotationally-averaged weak dipolar interactions between pairs or ensembles of spins under magic-angle spinning (MAS) play a valuable role in the structural analysis of organic and biomolecular solids [1–4]. Homonuclear (e.g., ^{13}C–^{13}C) and heteronuclear (e.g., ^{13}C–^{15}N) dipolar interactions can be manipulated to provide estimates of through-space internuclear distances and constraints on torsional angles relating pairs of dipolar vectors. Homonuclear recoupling under rotational resonance (R^2) has been exploited widely to measure distances in the structure determination of membrane proteins and other biomolecular solids, for example [5–7]. The nth order R^2 condition is met when the difference N_{IS} in the Larmor frequencies of a pair of spins is equal to the MAS frequency ν_R (i.e., $n = 1$) or an integer multiple thereof ($n \geqslant 2$) [8]. Mechanical rotation at R^2 prevents averaging of the dipolar interactions and zero-quantum coherences can be excited from an initial condition of difference polarization. Examination of the time dependence of exchange of Zeeman order provides estimates of distance-dependent coupling constants permitting measurements of distances of up to 6.8 Å for ^{13}C–^{13}C pairs, for example [9]. Selective ^{13}C–^{13}C distances have also been measured from uniformly ^{13}C-labelled solids under R^2 in cases where the couplings between the pair of interest are strong relative to the Larmor frequency separation from other spins [10,11].

Torsional angles defined by carbon, nitrogen and protons, such as N1–C1–C2–N2, H1–C1–C2–H2 and H1–C1–N2–H2, can be estimated in experiments exciting ^{13}C1–^{13}C2 double-quantum coherences or ^{13}C1–^{15}N1 multiple quantum coherences [12–15]. The evolution of the coherences under the influence of local dipolar fields generated by H1 and H2 or N1 and N2 is influenced by the relative orientations of the C–H and N–H bonds in a predictable manner. For selectively labelled solids signal amplitudes are measured in a series of one-dimensional experiments in which the double-quantum evolution period is varied. For extensively or uniformly ^{13}C- and/or ^{15}N-labelled solids, such as proteins, multidimensional experiments correlating double-quantum and single-quantum coherences are often necessary [12,16]. These experiments can be time consuming, however, and so it would be useful to selectively estimate individual torsional angles from uniformly labelled materials using a series of one-dimensional experiments.

Levitt and colleagues have described a method to excite double-quantum coherence under R^2, in which mechanically excited zero-quantum coherences are converted into double-quantum coherences by frequency-selective spin inversion [17]. Highly efficient excitation was achieved for solids labelled with strongly coupled ^{13}C spin pairs, but subsequent work has shown that the efficiency and selectivity can be somewhat poorer for uniformly ^{13}C-labelled solids in which there is considerable overlap of

* Corresponding author. Fax: +44 151 7954406.
E-mail address: middleda@liv.ac.uk (D.A. Middleton).

1090-7807/$ - see front matter © 2009 Elsevier Inc. All rights reserved.
doi:10.1016/j.jmr.2009.05.002

chemical shielding anisotropies and/or small differences in the isotropic chemical shifts [18,19]. Here we show that, in favourable circumstances, it is possible to obtain selectively double-quantum filtered ^{13}C spectra of uniformly labelled solids under R^2. By following the evolution of the selectively-excited double-quantum coherences under local proton fields we obtain reliable estimates of individual H–C–C–H torsional angles and projection angles relating the orientations of non-bonded C–H pairs.

2. Results and discussion

A pulse sequence adapted from Levitt and colleagues [17,20] is shown in Fig. 1, annotated here for the specific case of H–C–C–H angle measurements. The sample rotation frequency is adjusted to the $n = 1$ rotational resonance condition (i.e., $\nu_R = N_{IS}$) and the spectrometer reference frequency is set to the mean of the isotropic chemical shift frequencies for the ^{13}C spin pair of interest. After cross-polarization, ^{13}C magnetization lies along the x-axis of the rotating frame. After a delay δ, equal to $1/2N_{IS}$ for the spin pair of interest (and also equal to $1/2\nu_R$ at $n = 1$ R^2), a $\pi/2$ pulse creates longitudinal difference polarization, in which magnetization for one of the sites is stored along +z and magnetization for the other site is stored along $-z$. Zero-quantum coherence correlating the spin pair of interest is excited mechanically by sample rotation during the interval t_m, which is set to approximately the inverse of the dipolar coupling constant b_{CC}. Zero-quantum coherence is converted into double-quantum coherence by two $\pi/2$ pulses separated by delay δ. The double-quantum coherence then evolves for one rotor period ($t_R = 1/\nu_R$) under the influence of ^1H–^{13}C dipolar

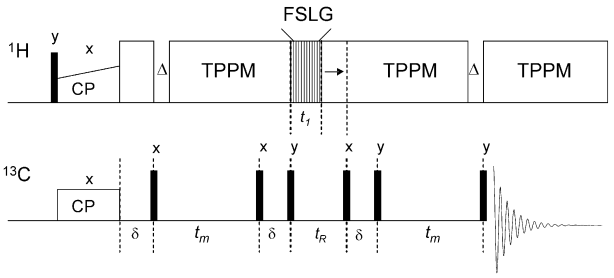

Fig. 1. Pulse sequence for selectively determining the relative orientations of pairs of heteronuclear dipolar vectors, C_i–H_i and C_j–H_j. Double-quantum coherences are excited at $n = 1$ rotational resonance and modulated under the influence of scaled C_i–H_i and C_j–H_j dipolar interactions during t_1. The effect of the isotropic ^{13}C chemical shifts over the evolution interval of one rotation period is removed by setting the radiofrequency carrier to the mean of the resonance frequencies for C_i and C_j. The proton transmitter is switched off for two delays Δ of 100 μs to dephase residual transverse components of the magnetization.

interactions. This is accomplished by effectively removing ^1H–^1H couplings from the beginning of this interval for a period t_1 (where $0 \leqslant t_1 \leqslant t_R$), here using the frequency-switched Lee-Goldberg method. Double-quantum coherence is then reconverted to zero-quantum coherence with a further $\pi/2$–δ–$\pi/2$ step and after a second t_m interval a final $\pi/2$ read-out pulse creates single-quantum coherence. Thus the ^{13}C coherences are manipulated by just six radiofrequency pulses. A standard 8-step phase cycle is applied to the pulses and to the receiver to eliminate unwanted coherences [17]. The double-quantum filtered spectrum ideally consists of two

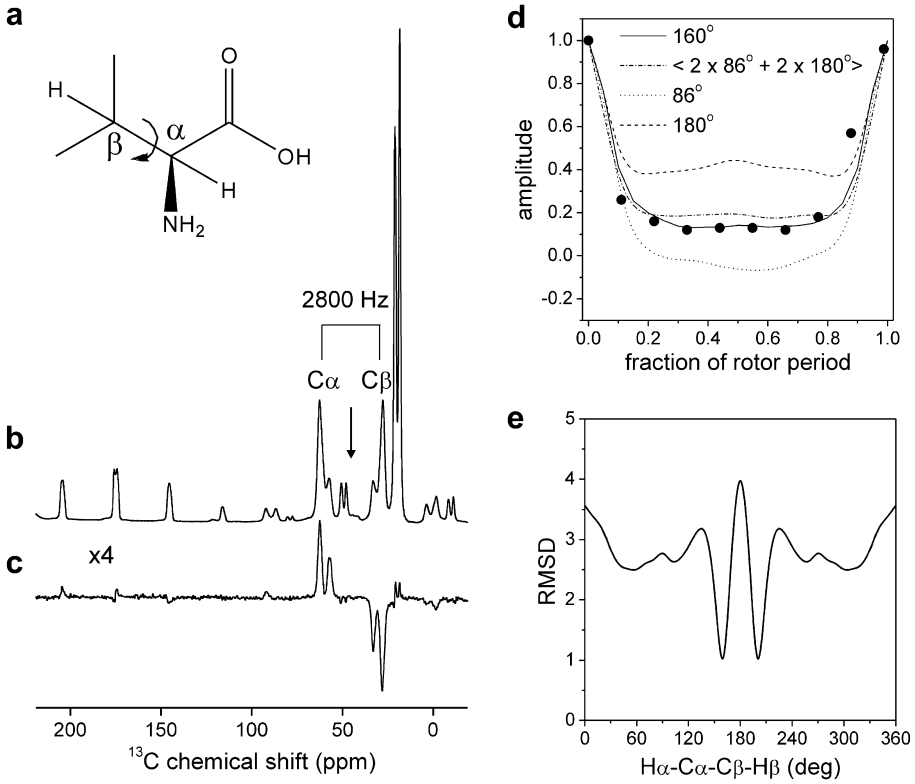

Fig. 2. Measurement of the torsional angle Hα–Cα–Cβ–Hβ (χ_1) for L-[U-^{13}C,^{15}N]valine. (a) Chemical structure of valine, highlighting the α and β positions. (b) A ^{13}C cross-polarization magic-angle spinning NMR spectrum from a 10 mg sample. (c) A spectrum obtained using the pulse sequence in Fig. 1 ($t_1 = 0$ and $t_m = 350$ μs). Both spectra are the result of averaging 64 transients. The MAS frequency of 2800 Hz is equivalent to N_{IS} for Cα and Cβ. The arrow denotes the spectrometer carrier frequency. (d) Signal amplitudes for Cα–Cβ double-quantum coherence as a function of the evolution period t_1. Normalized experimental data (circles) are overlaid with a simulated amplitude curve for a θ angle of ±160° (solid line), the best fitting curve for a single distance. Also shown are curves for the individual θ angles (86° and 180°) for each of the two pairs of conformationally distinct molecules in the asymmetric unit (dotted line and dashed line, respectively) and a curve for the two geometries averaged over the asymmetric unit (dotted-dashed line). (e) Root-mean-square deviation (RMSD) from the experimental data of curves simulated for different θ angles, showing the minimum at ±160°.

peaks for the coupled spin pair, one inverted relative to the other and with amplitudes modulated by the C–H dipolar interactions during t_1. In a series of experiments t_1 is varied from zero to t_R and the measured amplitudes are compared with numerical simulations to provide H–C–C–H angle estimates [14]. Experiments were performed on a Bruker Avance 400 spectrometer operating at 9.3 T and equipped with a Bruker triple resonance MAS probe with a 4 mm diameter sample rotor and tuned to 100.13 MHz for ^{13}C and 400.12 MHz for ^{1}H. In all experiments the cross-polarization contact time was 1 ms, the ^{13}C $\pi/2$ pulse lengths were 3.5 μs and the proton decoupling radiofrequency field was 100 kHz. The recycle delay was 2 ms for valine and 20 ms for uridine. After the cross-polarization step, two-pulse phase modulated (TPPM) decoupling [21] was applied throughout except during periods Δ and t_1.

The method is first demonstrated with L-[U-^{13}C,^{15}N]valine, obtained from Cambridge Isotope Laboratories and used without further preparation (Fig. 2a). The sample rotation frequency was adjusted to $\nu_R = 2800$ Hz (±2 Hz), which is $n = 1$ R^2 with respect to the resonance frequencies of the valine α-carbon (Cα) and β-carbon (Cβ). A mixing time of 350 μs was used, which is theoretically optimal for the Cα–Cβ dipolar coupling constant of 2 kHz. The normal cross-polarization ^{13}C spectrum (Fig. 2b) shows single peaks from all five carbons in valine and so does not distinguish between the two conformationally distinct molecules in the asymmetric unit [22]. The peaks for Cα and Cβ are clearly split into doublets consistent with the strong dipolar coupling between the spins. The double-quantum filtered spectrum (Fig. 2c) obtained using the pulse sequence in Fig. 1 (with $t_1 = 0$) effectively eliminates all but the signals for Cα and Cβ; the effect of strong coupling compensates for the small frequency separation and overlapping chemical shielding anisotropies. The excitation efficiency (25%) is somewhat lower than reported earlier for glycine, however [17]. The signal amplitudes for double-quantum evolution under C–H dipolar coupling are shown in Fig. 2d. Comparison with curves simulated numerically as a function of the Cα–Cβ–Hβ and Hα–Cα–Cβ bond angles, Cα–Cβ and C–H distances and different Hα–Cα–Cβ–Hβ torsional angles (defined here as θ) suggests at first inspection that the closest agreement is for an angle of ±160° (Fig. 2d, solid line, and Fig. 2e). The crystallographic asymmetric unit of valine contains two molecules with a gauche(+) conformation ($\theta = 86°$) and two molecules in a trans ($\theta = 180°$) conformation [22]. A curve simulated for these two geometries averaged across the asymmetric unit (i.e., $<2 \times 86° + 2 \times 180°>$) gives good agreement with the experimental data (Fig. 2d, dotted-dashed line).

A more challenging case is next shown in which the relative orientations of C–H bonds are estimated for a pair of non-bonded ^{13}C spins in uniformly labelled [^{13}C,^{15}N] uridine (obtained from Cambridge Isotope Laboratories and co-crystallized from water with 90% unlabelled uridine). The relative orientations of the pyrimidine and ribose rings is defined by the torsional angle C6–N1–C1′–H1′ (Fig. 3a), which cannot be measured directly by NMR. The C6–N1–C1′–H1′ angle is geometrically related to the relative orientation of the H6–C6 and C1′–H1′ bonds, however (Fig. 3b). The H6–C6–C1′–H1′ projection angle can in principle be measured using the pulse sequence in Fig. 1 provided double-quantum coherence can be excited selectively for the nonbonded spins C6 and C1′. The angle C6–C1′–H1′ also varies systematically with C6–N1–C1′–H1′ (Fig. 3b) and this must be taken into consideration when numerically simulating curves for comparison with the experimental data. Fig. 4a shows the normal cross-polarization ^{13}C spectrum of 10% uniformly labelled [^{13}C,^{15}N]uridine obtained with a MAS frequency $\nu_R = 5200$ Hz, which is the $n = 1$ rotational resonance frequency with respect to C6 and C1′. The peaks for C6 and C1′ are broadened slightly but not split as in valine, because

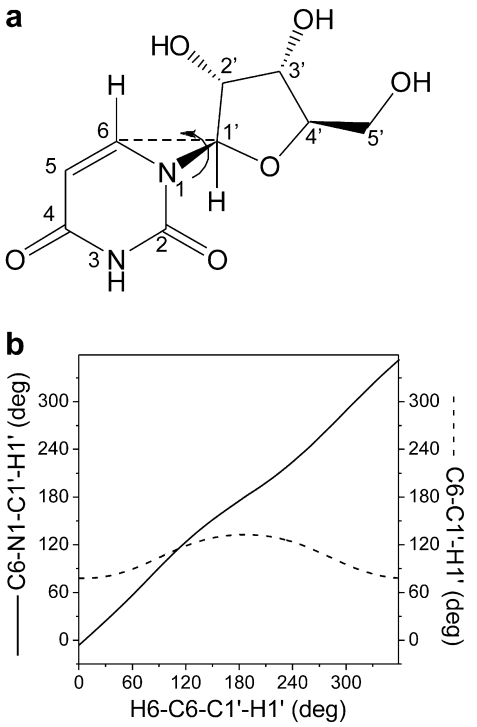

Fig. 3. The molecular geometry of uridine. (a) Chemical structure and numbering system. The rotational freedom of the N1–C1′ bond is indicated by an arrow. The dotted line between C6 and C1′ and the bonded hydrogen atoms are shown to highlight the effective torsional angle H6–C6–C1′–H1′. (b) Relationship between the projection angle H6–C6–C1′–H1′ measured by NMR and the torsional angle C6–N1–C1′–H1′ and effective bond angle C6–C1′–H1′.

the ^{13}C–^{13}C internuclear distance of 2.5 Å gives rise to weaker dipolar coupling ($b_{CC} = 486$ Hz). The doubling of several of the peaks is consistent with an asymmetric unit comprising two conformationally distinct molecules, as evident in the X-ray crystal structure [23]. The efficiency of double-quantum filtration using the pulse sequence in Fig. 1 (with $t_1 = 0$ and $t_m = 1.45$ ms) is rather low (12%), consistent with the weak coupling between the C6 and C1′ spins. The double-quantum filter nevertheless achieves excellent selectivity for C6 and C1′, despite the substantial overlap in their chemical shielding anisotropies (Fig. 4b). The double-quantum filter effectively excludes coherences between C5 and C6, which are bonded to each other and thus strongly coupled, because the MAS frequency is 1.2 kHz above the rotational resonance condition with respect to this spin pair. The MAS frequency is close to the $n = 1$ R^2 condition for only one other spin pair (C2 and C5), but signals from these spins are also filtered from the spectrum, presumably because t_m is not optimised for the C2–C5 coupling constant (346 Hz).

The measured signal amplitudes for C6 and C1′ double-quantum evolution under the C–H dipolar interaction are in excellent agreement with a calculated curve representing a superposition of the H6–C6–C1′–H1′ angles (139° and 144°) defining the two known geometries in the asymmetric unit (Fig. 4c). To illustrate the precision with which the uridine geometry can be estimated from the experimental amplitudes, Fig. 4d shows the deviation from the data of curves calculated for the full range of the H6–C6–C1′–H1′ projection angles. Closest agreement occurs for H6–C6–C1′–H1′ projection angles of between 135° and 220° (Fig. 4d), which from Fig. 3b correspond to C6–N1–C1′–H1′ angles of between 143° and 206°. The NMR data thus constrains the relative orientations of the pyrimidine and ribose rings within less than a quadrant of the entire conformational range (Fig. 4e).

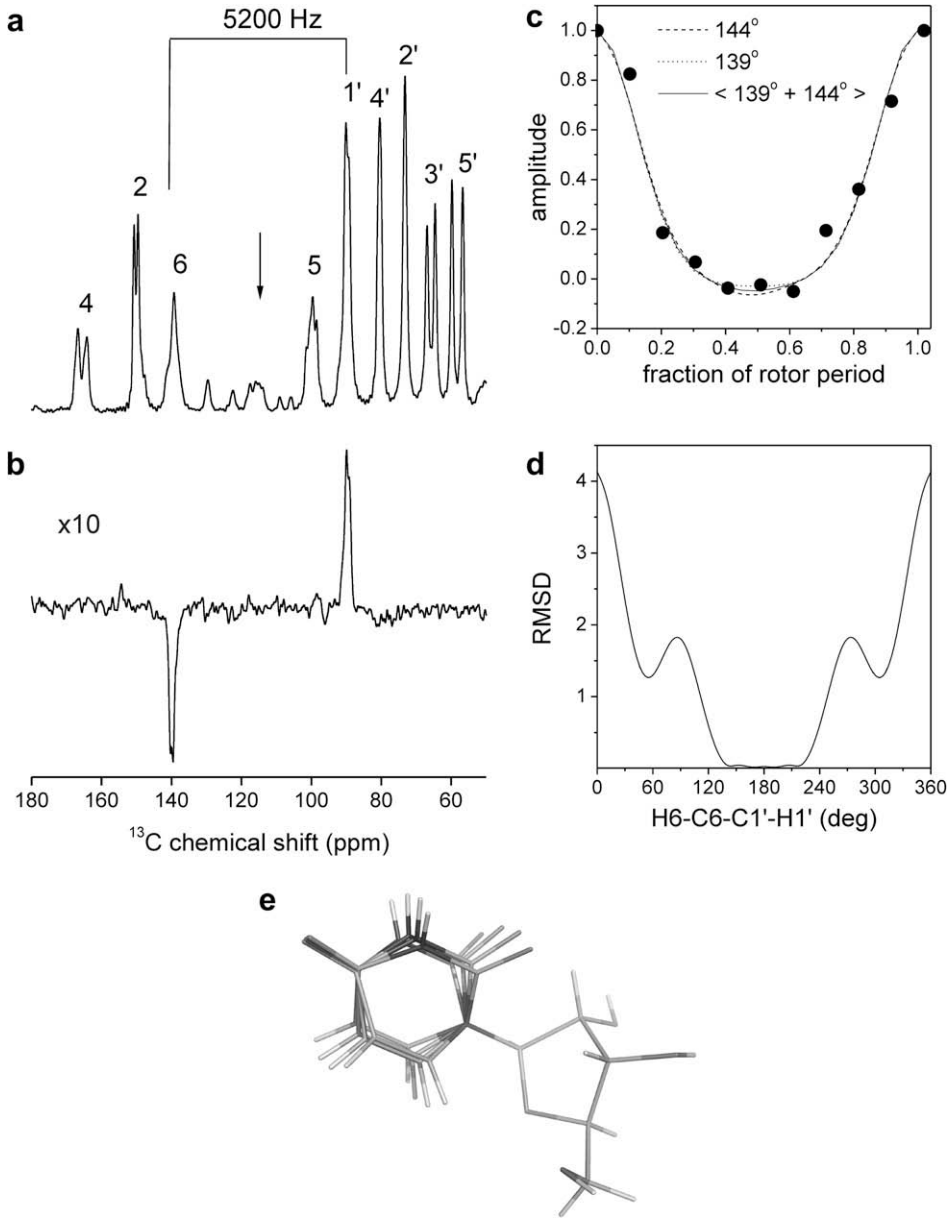

Fig. 4. Measurement of the effective torsional angle H6–C6–C1′–H1′ for uniformly labelled 10% [^{13}C,^{15}N]uridine (5 mg). The MAS frequency of 5200 Hz is equivalent to N_{IS} for C6 and C1′. The arrow denotes the spectrometer carrier frequency. (a) A ^{13}C cross-polarization magic-angle spinning NMR spectrum. (b) A spectrum obtained using the pulse sequence in Fig. 1 (t_1 = 0 and t_m = 1.45 ms). Both spectra are the result of averaging 2048 transients. (c) Signal amplitudes for Cα–Cβ double-quantum coherence as a function of the evolution period t_1. Normalized experimental data (circles) are overlaid with curves calculated for individual H6–C6–C1′–H1′ angles of 139° and 144° measured from the crystal structure, and with a curve representing both molecular geometries averaged across the asymmetric unit. (d) RMSD from the experimental data of curves simulated for H6–C6–C1′–H1′ projection angles spanning the entire possible conformational range of uridine. (e) An ensemble of uridine conformations corresponding to the RMSD minima for angles between 135° and 220°.

3. Conclusions

In summary it is shown that it is possible to selectively excite double-quantum coherences within uniformly ^{13}C-labelled solids. Coherences excited under rotational resonance can be exploited to estimate individual torsional angles or projection angles by performing a series of one-dimensional experiments measuring proton-modulated signal amplitudes. Although in the examples described there is some overlap of chemical shielding anisotropies for the recoupled spins, this does not appear to compromise selectivity in these instances. It should be mentioned that the selectivity and efficiency of the double-quantum filter is highly sample dependent, however. For many compounds unwanted coherences may be excited if resonance lines for weakly coupled spins are close to lines for strongly coupled spins, or if additional spin pairs are recoupled near or at higher order rotational resonance [18,19]. Overlapping shielding tensors may also affect selectivity and efficiency of the double-quantum filter. Alternative schemes with radiofrequency-assisted excitation of selective coherences away from R^2 may be useful in such cases [20,24,25], as may alternative procedures for selective spin inversion.

Acknowledgments

This work was funded by the BBSRC (studentship to RE), the EPSRC (EP/C00664X/1) and the EU European Membrane Protein consortium (E-MeP, contract LSHG-CT-2004-504601). SGP thanks Peter Henderson (University of Leeds) for support.

References

[1] C.P. Jaroniec, C.E. MacPhee, V.S. Bajaj, M.T. McMahon, C.M. Dobson, R.G. Griffin, High-resolution molecular structure of a peptide in an amyloid fibril determined by magic angle spinning NMR spectroscopy, Proc. Natl. Acad. Sci. USA 101 (2004) 711–716.

[2] C.P. Jaroniec, C. Filip, R.G. Griffin, 3D TEDOR NMR experiments for the simultaneous measurement of multiple carbon-nitrogen distances in uniformly C-13, N-15-labeled solids, J. Am. Chem. Soc. 124 (2002) 10728–10742.

[3] J.M. Goetz, J. Schaefer, REDOR dephasing by multiple spins in the presence of molecular motion, J. Magn. Reson. 127 (1997) 147–154.

[4] A.T. Petkova, Y. Ishii, J.J. Balbach, O.N. Antzutkin, R.D. Leapman, F. Delaglio, R. Tycko, A structural model for Alzheimer's beta-amyloid fibrils based on experimental constraints from solid state NMR, Proc. Natl. Acad. Sci. USA 99 (2002) 16742–16747.

[5] J.M. Griffiths, T.T. Ashburn, M. Auger, P.R. Costa, R.G. Griffin, P.T. Lansbury, Rotational resonance solid-state NMR elucidates a structural model of pancreatic amyloid, J. Am. Chem. Soc. 117 (1995) 3539–3546.

[6] F. Creuzet, A. McDermott, R. Gebhard, K. Vanderhoef, M.B. Spijkerassink, J. Herzfeld, J. Lugtenburg, M.H. Levitt, R.G. Griffin, Determination of membrane-protein structure by rotational resonance NMR – bacteriorhodopsin, Science 251 (1991) 783–786.

[7] S.O. Smith, B.J. Bormann, Determination of helix–helix interactions in membranes by rotational resonance NMR, Proc. Natl. Acad. Sci. USA 92 (1995) 488–491.

[8] D.P. Raleigh, M.H. Levitt, R.G. Griffin, Rotational resonance in solid-state NMR, Chem. Phys. Lett. 146 (1988) 71–76.

[9] O.B. Peersen, S. Yoshimura, H. Hojo, S. Aimoto, S.O. Smith, Rotational resonance NMR measurements of internuclear distances in an alpha-helical peptide, J. Am. Chem. Soc. 114 (1992) 4332–4335.

[10] P.T.F. Williamson, A. Verhoeven, M. Ernst, B.H. Meier, Determination of internuclear distances in uniformly labeled molecules by rotational-resonance solid-state NMR, J. Am. Chem. Soc. 125 (2003) 2718–2722.

[11] P.T.F. Williamson, A. Verhoeven, K.W. Miller, B.H. Meier, A. Watts, The conformation of acetylcholine at its target site in the membrane-embedded nicotinic acetylcholine receptor, Proc. Natl. Acad. Sci. USA 104 (2007) 18031–18036.

[12] V. Ladizhansky, C.P. Jaroniec, A. Diehl, H. Oschkinat, R.G. Griffin, Measurement of multiple psi torsion angles in uniformly C-13, N-15-labeled alpha-spectrin SH3 domain using 3D N-15-C-13-C-13-N-15 MAS dipolar-chemical shift correlation spectroscopy, J. Am. Chem. Soc. 125 (2003) 6827–6833.

[13] P.R. Costa, J.D. Gross, M. Hong, R.G. Griffin, Solid-state NMR measurement of Psi in peptides: a NCCN 2Q-heteronuclear local field experiment, Chem. Phys. Lett. 280 (1997) 95–103.

[14] X. Feng, Y.K. Lee, D. Sandstrom, M. Eden, H. Maisel, A. Sebald, M.H. Levitt, Direct determination of a molecular torsional angle by solid-state NMR, Chem. Phys. Lett. 257 (1996) 314–320.

[15] X. Feng, P.J.E. Verdegem, Y.K. Lee, D. Sandstrom, M. Eden, P. BoveeGeurts, W.J. deGrip, J. Lugtenburg, H.J.M. deGroot, M.H. Levitt, Direct determination of a molecular torsional angle in the membrane protein rhodopsin by solid-state NMR, J. Am. Chem. Soc. 119 (1997) 6853–6857.

[16] C.M. Rienstra, M. Hohwy, L.J. Mueller, C.P. Jaroniec, B. Reif, R.G. Griffin, Determination of multiple torsion-angle constraints in U-C-13, N-15-labeled peptides: 3D H-1-N-15-C-13-H-1 dipolar chemical shift NMR spectroscopy in rotating solids, J. Am. Chem. Soc. 124 (2002) 11908–11922.

[17] T. Karlsson, M. Eden, H. Luthman, M.H. Levitt, Efficient double-quantum excitation in rotational resonance NMR, J. Magn. Reson. 145 (2000) 95–107.

[18] M. Bechmann, X. Helluy, A. Sebald, Double-quantum-filtered rotational-resonance MAS NMR in the presence of large chemical shielding anisotropies, J. Magn. Reson. 152 (2001) 14–25.

[19] S. Dusold, A. Sebald, Double-quantum filtration under rotational-resonance conditions: numerical simulations and experimental results, J. Magn. Reson. 145 (2000) 340–356.

[20] T. Karlsson, C.E. Hughes, J. Gunne, M.H. Levitt, Double-quantum excitation in the NMR of spinning solids by pulse-assisted rotational resonance, J. Magn. Reson. 148 (2001) 238–247.

[21] A.E. Bennett, C.M. Rienstra, M. Auger, K.V. Lakshmi, R.G. Griffin, Heteronuclear decoupling in rotating solids, J. Chem. Phys. 103 (1995) 6951–6958.

[22] K. Torii, Y. Iitaka, The crystal structure of L-valine, Acta Crystallogr. B26 (1970) 1317–1326.

[23] E.A. Green, R.D. Rosenstein, R. Shiono, D.J. Abraham, B.L. Trus, R.E. March, The crystal structure of uridine, Acta Crystallogr. B31 (1975) 102–107.

[24] K. Takegoshi, K. Nomura, T. Terao, Rotational resonance in the tilted rotating-frame, Chem. Phys. Lett. 232 (1995) 424–428.

[25] K. Takegoshi, K. Nomura, T. Terao, Selective homonuclear polarization transfer in the tilted rotating frame under magic angle spinning in solids, J. Magn. Reson. 127 (1997) 206–216.